Journal of ELECTRONIC MATERIALS, Vol. 39, No. 4, 2010
DOI: 10.1007/s11664-010-1093-8

Additive Occupancy in the Cu_6Sn_5-Based Intermetallic Compound Between Sn-3.5Ag Solder and Cu Studied Using a First-Principles Approach

FENG GAO,[1,2,4] JIANMIN QU,[1,2] and TADASHI TAKEMOTO[3]

1.—George W. Woodruff School of Mechanical Engineering, Georgia Institute of Technology, Atlanta 30332-0405, USA. 2.—McCormick School of Engineering and Applied Science, Northwestern University, 2145 Sheridan Road, Evanston 60208, USA. 3.—Joining and Welding Research Institute, Osaka University, Osaka 567-0047, Japan. 4.—e-mail: feng-gao@northwestern.edu

A Cu_6Sn_5-based intermetallic compound containing a certain amount of Co or Ni is commonly formed at the interface between a Cu substrate and Sn-based solder. The Co or Ni additive is often found to occupy the Cu atom sublattice in the Cu_6Sn_5 crystal structure. In this paper, a first-principles approach based on density-functional theory is employed to explore the most favorable occupancy sites of Ni and Co dopants in the Cu_6Sn_5 crystal structure. It is found that, for up to 27.3 at.% concentration, both Ni and Co atoms tend to substitute for Cu in the Cu_6Sn_5-based structure and form more thermodynamically stable $(Cu,Ni)_6Sn_5$ and $(Cu,Co)_6Sn_5$ phases. In comparison, Ni is more effective than Co at stabilizing the Cu_6Sn_5 phase. At a lower concentration level (9.1 at.%), the Ni or Co atoms prefer to occupy the 4e Cu sublattice. At a higher concentration (27.3 at.%), the Ni atoms will likely be located on the 4e + 8f2 Cu sublattice. Analysis of density of states (DOS) and partial density of states (PDOS) indicates that hybridization between Ni-*d* (or Co-*d*) and Sn-*p* states plays a dominant role in structural stability. Compared with $Cu_4Ni_2Sn_5$, where Ni occupies the 8f2 Cu sublattice, $Cu_4Co_2Sn_5$ is less stable due to the lower amplitude of the Co-*d* PDOS peak and its position mismatch with the Sn-*p* PDOS peak.

Key words: Solder, intermetallic compounds, additive, first principles, density of states

INTRODUCTION

Organic solderability preservative (OSP) is a common coating on Cu pads in current electronic packaging. During solder reflow, the Cu_6Sn_5 intermetallic compound (IMC) is usually formed at the interface between Sn-based solder and OSP.[1] The Cu_6Sn_5 IMC serves as a metallurgical and thermo/electroconductive media in the solder interconnections. It has been reported that the Cu_6Sn_5-based phase typically contains a certain amount of Ni due to the interfacial reaction between solder and the metallization.[2–5] Chen et al. have reported that a large Ni solubility is found in the Cu_6Sn_5-based intermetallic compound.[2,3] In particular, Ghosh has found that the addition of Ni does not alter the crystal type of Cu_6Sn_5 because the Ni atoms substitute for the Cu atoms in the crystal structure.[4,5] These findings have been further confirmed by other researchers.[6–12] Similarly, the Co additive in the Sn-based lead-free solders shows the same behavior.[13] In other words, the Cu_6Sn_5 phase containing Co or Ni doping atoms can be labeled as $(Cu,Co)_6Sn_5$ and $(Cu,Ni)_6Sn_5$, respectively. Regarding Ni solubility in the Cu_6Sn_5 phase, Laurila et al. have reported that a $Cu_{29}Ni_{26}Sn_{45}$ stable ternary phase can be formed after a long annealing time (up to 10,000 h).[6,10,12] Furthermore, a $(Cu,Ni)_6Sn_5$ ternary

(Received August 10, 2009; accepted January 11, 2010; published online February 24, 2010)

phase with Ni solubility of 23.5 at.% was observed by Kao and coworkers,[7,11] and a Cu_6Sn_5 phase bearing 26.23 at.% Ni solubility was found by Chen et al.[3] Regarding Co solubility in $(Cu,Co)_6Sn_5$, few research works have been reported. The measured Co concentration in $(Cu,Co)_6Sn_5$, which is formed between Cu and Sn-3.5Ag solder containing a small amount of Co additive, is about 8.0 at.%.[13]

It has been speculated that both $(Cu,Co)_6Sn_5$ and $(Cu,Ni)_6Sn_5$ phases possess a similar crystal microstructure to Cu_6Sn_5, in which Co or Ni atoms occupy the Cu atom sublattice.[4,5,13] However, the crystal microstructure of $(Cu,Co)_6Sn_5$ and $(Cu,Ni)_6Sn_5$ phases have not been studied extensively. Works in this area include atomic-level simulation based on density-functional theory (DFT) to study the effects of dopants on the properties of other IMCs.[14,15] Such *ab initio* simulations have also been conducted to calculate the structural and mechanical properties of Cu_6Sn_5, $(Cu,Ni)_6Sn_5$, Ni_3Sn_4, and Cu_3Sn IMCs.[16–20] However, few works have been reported on the $(Cu,Co)_6Sn_5$ phase. In addition, $(Cu,Ni)_6Sn_5$ with a higher Ni concentration (around 26 at.%) has been reported but has not been investigated. This paper is devoted to address these issues by exploring the thermodynamic and electronic structure properties of the $(Cu,Co)_6Sn_5$ and $(Cu,Ni)_6Sn_5$ phases. The Cu_6Sn_5 phase is also calculated for comparison.

$(Cu,Co)_6Sn_5$ AND $(Cu,Ni)_6Sn_5$ MODEL SIMULATIONS

Larsson et al.[21] showed that the crystal microstructure of the Cu_6Sn_5 phase is monoclinic (space group *C*2/*c*, no. 15). The Cu_6Sn_5 unit cell consists of 24 Cu atoms and 20 Sn atoms. The Cu atoms occupy the 4a, 4e, and two different 8f sites (8f1 and 8f2), while the Sn atoms are located on the 4e and two different 8f sites (8f1 and 8f2). Figure 1a illustrates a unit cell of Cu_6Sn_5 with the atoms labeled by space site; that is, the Cu1, Cu2, Cu3, and Cu4 atoms are located at the 4a, 4e, 8f1, and 8f2 space sites, respectively, and the Sn1, Sn2, and Sn3 atoms occupy the 4e, 8f1, and 8f2 space sites, respectively. The initial lattice constants of the Cu_6Sn_5 unit cell for our simulation are a = 10.8002 Å, b = 7.1786 Å, c = 9.6907 Å, and β = 98.58°.

In order to perform first-principles calculations, the following simulation models were constructed in the current study. For the $(Cu,Co)_6Sn_5$ phase, the Cu atoms at the 4a or 4e sites were replaced by Co atoms. The formula is thus $Cu_5Co_1Sn_5$. Furthermore, the Cu atoms at the (4a + 4e), 8f1 or 8f2 sites were replaced by Co atoms, leading to a formula resembling $Cu_4Co_2Sn_5$. A similar method was used to create the $Cu_5Ni_1Sn_5$ and $Cu_4Ni_2Sn_5$ phases. In addition, phases with the formulas $Cu_3Co_3Sn_5$ and $Cu_3Ni_3Sn_5$ were also generated by replacing the (4e + 8f2) or (4a + 8f2) Cu sublattice to resemble the $(Cu,Co)_6Sn_5$ and $(Cu,Ni)_6Sn_5$ phases, with a higher

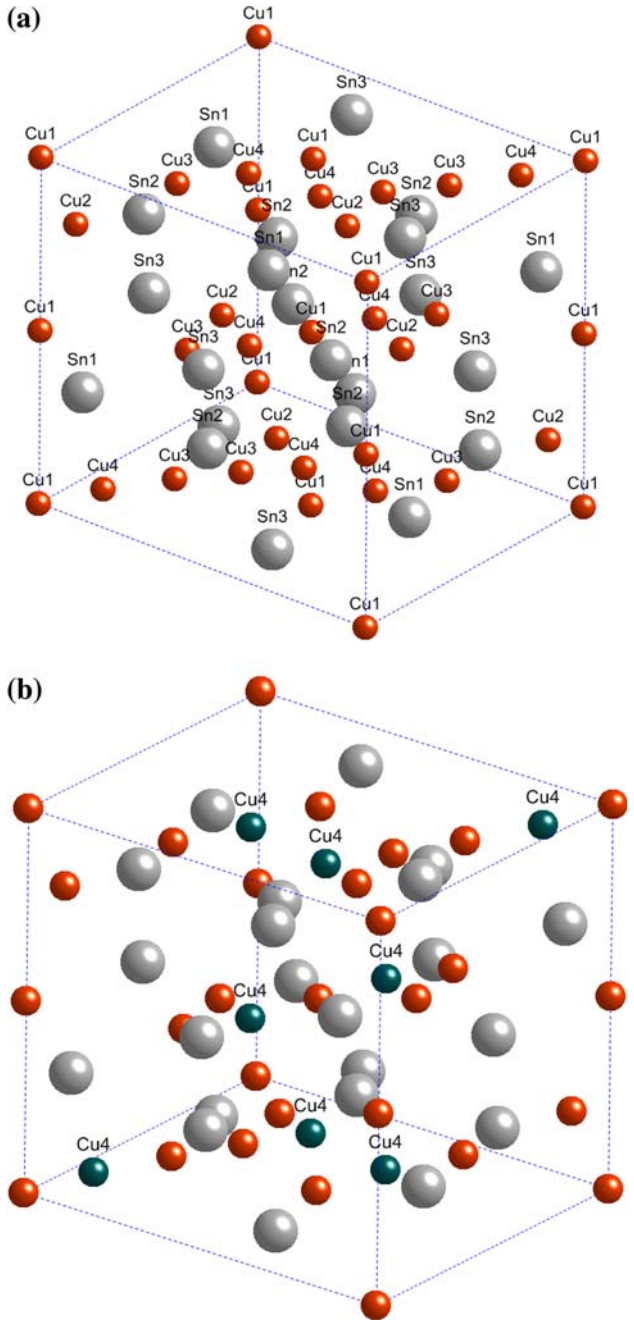

Fig. 1. Unit cell of Cu_6Sn_5 (monoclinic, space *C*2/*c*, no. 15): (a) Cu_6Sn_5 unit cell configuration: small red spheres represent Cu atoms, and larger grey spheres represent Sn atoms; (b) Cu atoms at the 8f2 sublattice to be replaced by Ni or Co atoms.

Co or Ni concentration (27.3 at.%). Figure 1b illustrates the atoms at the 8f2 Cu sublattice that are to be replaced by the Ni or Co atoms to form the $Cu_4Ni_2Sn_5$ or $Cu_4Co_2Sn_5$ phases, respectively.

First-principles simulations for periodic-boundary systems were performed using the *ab initio* pseudopotential theory. All calculations were conducted based on the generalized gradient approximation with the Perdew-Burke-Ernzerhof (GGA-PBE) pseudopotential. The CASTEP code (Materials

Studio)[22,23] was employed to carry out the atomic simulation with a plane-wave basis-set cutoff of 300.0 eV. The pseudo-atomic calculation was performed for the following electron configurations: $3d^{10}4s^1$ of Cu, $5s^25p^2$ of Sn, $3d^84s^2$ of Ni, and $3d^74s^2$ of Co. The non-spin-polarized Hamiltonian was employed in this study. All cell systems were optimized geometrically before calculation. An energy criterion was used for convergence, with a total energy tolerance of 1×10^{-5} eV and eigenenergy tolerance of 1×10^{-6} eV. The primitive cell-based supercell structure was used in order to reduce computation time.

SIMULATION RESULTS AND DISCUSSION

First, the total energy of the Cu_6Sn_5-based IMC was calculated as a function of cell volume based on the first-principles approach. Then, the total energy was utilized to extract the heat of formation of the Cu_6Sn_5, $(Cu,Ni)_6Sn_5$, and $(Cu,Co)_6Sn_5$ phases. The heat of formation is related to the composition-average energies of the pure component elements in their equilibrium crystal structure.[24] Therefore, for the formula $Cu_mX_nSn_k$ (X = Ni or Co), the heat of formation at zero temperature is

$$\Delta E = \frac{1}{m+n+k}\left[E^{\text{total}}_{Cu_mX_nSn_k} - (mE_{Cu} + nE_X + kE_{Sn})\right], \quad (1)$$

where ΔE is the heat of formation, $E^{\text{total}}_{Cu_mX_nSn_k}$ is the total energy of $Cu_mX_nSn_k$ (X = Ni or Co), and E_{Cu}, E_X, and E_{Sn} are the energies for the elements Cu, X (X = Ni or Co), and Sn, respectively. In this study, Cu has the face-centered cubic structure, and Sn is taken to have the β-Sn crystal structure. Similarly, Ni has the face-centered cubic structure, while Co has the hexagonal crystal structure. According to Eq. 1 and the calculated total energies, the heat of formation of the Cu_6Sn_5, $(Cu,Ni)_6Sn_5$, and $(Cu,Co)_6Sn_5$ phases was derived and is presented in Table I. As expected, the heat of formation of all phases is negative.

As shown in Table I, the calculated heat of formation for the Cu_6Sn_5 phase is −54.1 meV/atom. This value is between the experimentally measured value of −70 meV/atom[24] and the calculated values of −40.20 meV/atom (local density approximation, LDA) and −32.05 meV/atom (GGA) using the VASP code.[16] The values obtained using the CALPHAD method at 298 K based on the experimental data of Ref. 24 are −71.3 meV/atom to −77.5 meV/atom.[25–27] Clearly, our calculation results are in reasonable agreement with the existing literature values.

It follows from Table I that the additive in the Cu_6Sn_5 structure shows different effects on the phase stability depending on the dopant concentration and its occupancy sites. In general, at the same concentration, the $Cu_mNi_nSn_5$ phase is more stable than the $Cu_mCo_nSn_5$ phase. Moreover, the stability of $Cu_mNi_nSn_5$ and $Cu_mCo_nSn_5$ depends strongly on the dopant occupancy sites. For the $Cu_5Ni_1Sn_5$ formula, the Ni atoms prefer to occupy the 4e Cu sublattice. Increasing the Ni content in the Cu_6Sn_5-based phases (e.g., $Cu_4Ni_2Sn_5$ and $Cu_3Ni_3Sn_5$) further enhances the phase stability, as the absolute value of the heat of formation continues to increase. The Ni atoms prefer to occupy the 8f2 Cu sublattice in $Cu_4Ni_2Sn_5$, rather than the (4a + 4e) or 8f1 Cu sublattice, according to the heat of formation values given in Table I. In addition, the Ni atoms prefer to occupy the (4e + 8f2) Cu sublattice in $Cu_3Ni_3Sn_5$, rather than the (4a + 8f2) Cu sublattice. This also indicates that the $(Cu,Ni)_6Sn_5$ phase (Ni = 27.3 at.%) is a stable structure, which is consistent with the experimental observations.[3,6,7,9–12]

Co in $Cu_mCo_nSn_5$ behaves somewhat differently from Ni. Generally, the Co occupancy at the Cu sublattice leads to a more stable phase than Cu_6Sn_5. It is seen that the Co atoms prefer to occupy the 4e Cu sublattice in $Cu_5Co_1Sn_5$. For $Cu_4Co_2Sn_5$, the Co atoms can only occupy the 8f1 Cu sublattice, as occupancy at the (4a + 4e) or 8f2 Cu sublattice would lead to a less stable phase than $Cu_5Co_1Sn_5$ (Co at the 4e Cu sublattice). Similarly, at a high Co concentration level (i.e., 27.3 at.%), the favorable site of Co atoms is the (4e + 8f2) Cu sublattice.

To further understand the formation mechanisms, the electronic properties of five phases with formula Cu_6Sn_5, $Cu_5Ni_1Sn_5$ (Ni at 4e), $Cu_5Co_1Sn_5$ (Co at 4e), $Cu_4Ni_2Sn_5$ (Ni at 8f2), and $Cu_4Co_2Sn_5$ (Co at 8f2) were analyzed based on the density of states (DOS) and partial density of states (PDOS). The density of states (DOS) describes the number of

Table I. Heat of formation of Cu_6Sn_5, $(Cu,Ni)_6Sn_5$, and $(Cu,Co)_6Sn_5$ by first-principles calculation

	Additive Occupancy at Cu Sublattice	Heat of Formation (eV/atom)
Cu_6Sn_5	n/a	−0.0541
$Cu_5Co_1Sn_5$	Co = 4a	−0.0836
	Co = 4e	−0.1195
$Cu_4Co_2Sn_5$	Co = 4a + 4e	−0.1168
	Co = 8f1	−0.1236
	Co = 8f2	−0.1127
$Cu_3Co_3Sn_5$	Co = 4a + 8f2	−0.1168
	Co = 4e + 8f2	−0.1341
$Cu_5Ni_1Sn_5$	Ni = 4a	−0.1132
	Ni = 4e	−0.1332
$Cu_4Ni_2Sn_5$	Ni = 4a + 4e	−0.1645
	Ni = 8f1	−0.1677
	Ni = 8f2	−0.1682
$Cu_3Ni_3Sn_5$	Ni = 4a + 8f2	−0.1909
	Ni = 4e + 8f2	−0.2127

Pure Cu has the face-centered cubic structure, and Sn is taken to have the β-Sn crystal structure. Pure Ni has the face-centered cubic structure, while Co has the hexagonal crystal structure.

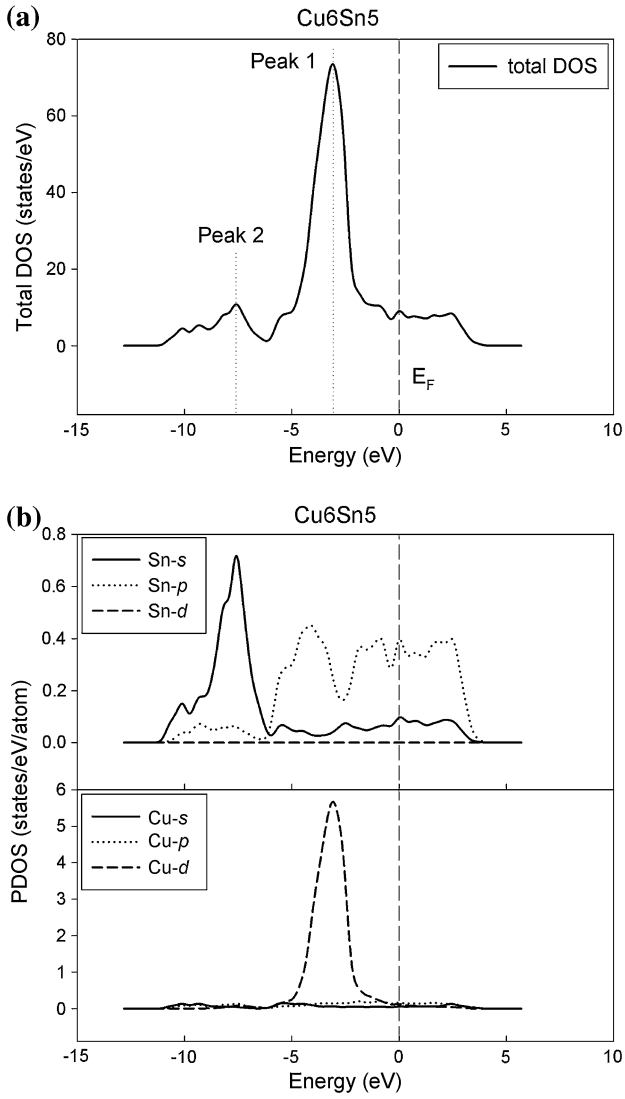

Fig. 2. Total density of states (DOS) of the Cu_6Sn_5 phase, and partial density of states (PDOS) of the Cu and Sn states. The Fermi level E_F is located at 0 eV: (a) total DOS; (b) PDOS of the Cu and Sn states.

states at each energy level that are available to be occupied, while the partial density of states (PDOS) illustrates the partial contributions from the component elements in the system.

Figure 2a and b illustrates the total density of states of the Cu_6Sn_5 phase, as well as the PDOS of the Cu and Sn states, respectively. In Fig. 2a, two peaks appear at energy levels of −3.20 eV and −7.77 eV, respectively. According to the PDOS results in Fig. 2b, the peak at −3.20 eV is mainly contributed by the Cu-*d* state, while the peak at −7.77 eV is mainly due to the contribution from the Sn-*s* state. Furthermore, for the Cu atoms in Cu_6Sn_5, the Cu-*s* and Cu-*p* states govern the valence bands at an energy lower than −7.0 eV, while the Cu-*d* state is dominant at an energy from −7 eV to 0 eV. In particular, the Cu-*d* state which is dominant at the energy level of −3.20 eV contributes to the bonding in the Cu_6Sn_5 crystal structure.[18] At the Fermi level (E_F = 0 eV), the contribution from the Sn-*p* state is greater than those from the *s*, *p*, and *d* states of Cu.

Figure 3a illustrates the total DOS of the Cu_6Sn_5-based phases due to the occupancy of Ni or Co at the 4e Cu sublattice, which corresponds to the $Cu_5Ni_1Sn_5$ and $Cu_5Co_1Sn_5$ formulas, respectively. The Co and Ni occupancy at the 4e Cu sublattice in Cu_6Sn_5 results in a second, weaker DOS peak at a position close to the Fermi level, compared with Cu_6Sn_5 in Fig. 2a. For $Cu_5Co_1Sn_5$ the amplitude of this second, weaker DOS peak is lower than that of $Cu_5Ni_1Sn_5$. Figure 3b shows the partial density of states (PDOS) of the Cu, Ni, and Sn states in $Cu_5Ni_1Sn_5$, while Fig. 3c depicts the PDOS of the Cu, Co, and Sn states in $Cu_5Co_1Sn_5$. Clearly, hybridization is demonstrated between Ni-*d* and Sn-*p* states at the energy level of −1.99 eV, as well as between Co-*d* and Sn-*p* states at the energy level of −1.53 eV. This is believed to be the dominant factor enhancing the stability of $Cu_5Ni_1Sn_5$ and $Cu_5Co_1Sn_5$, which is consistent with the Ni-Sn intermetallic stability study by Ghosh.[28] In addition, as shown in Fig. 3b and c, hybridization also takes place between Ni-*d* and Cu-*d* states (at the energy level of −3.29 eV), as well as between Co-*d* and Cu-*d* states (at the energy level of −3.25 eV). This hybridization also contributes to better stability of $Cu_5Ni_1Sn_5$ and $Cu_5Co_1Sn_5$ than Cu_6Sn_5.[18] The higher stability of $Cu_5Ni_1Sn_5$ than $Cu_5Co_1Sn_5$ may be attributed to the following two aspects: (1) the Ni-*d* PDOS peak amplitude is greater than that of the Co-*d* state, and (2) the total DOS of $Cu_5Co_1Sn_5$ (9.86 states/eV) at the Fermi level (E_F = 0 eV) is much larger than that of $Cu_5Ni_1Sn_5$ (7.99 states/eV), as shown in Fig. 3a. It has been reported that the phase stability of intermetallic compounds is closely related to the location of the Fermi level and the value of the DOS at the Fermi level.[29] A lower total DOS value at the Fermi level represents a more stable electronic structure.

Figure 4a shows the total density of states (DOS) of the $Cu_4Ni_2Sn_5$ and $Cu_4Co_2Sn_5$ phases in which the Ni or Co atoms substitute for Cu at the 8f2 sublattice. The total DOS of Cu_6Sn_5 is also presented for comparison. Similarly, another, weaker peak is also formed at the energy level between the Fermi level E_F and the first peak. For the $Cu_4Ni_2Sn_5$ phase, this second, weaker peak appears at the energy level of −1.60 eV, and it shifts to −0.92 eV for the $Cu_4Co_2Sn_5$ phase. Figure 4b illustrates the PDOS of the Cu, Ni, and Cu states in $Cu_4Ni_2Sn_5$, while Fig. 4c shows the PDOS of the Cu, Co, and Cu states in $Cu_4Co_2Sn_5$. It can be seen that the PDOS peak amplitude contributed by the Ni-*d* state is much greater than that contributed by the Co-*d* state. For the $Cu_4Ni_2Sn_5$ phase, the

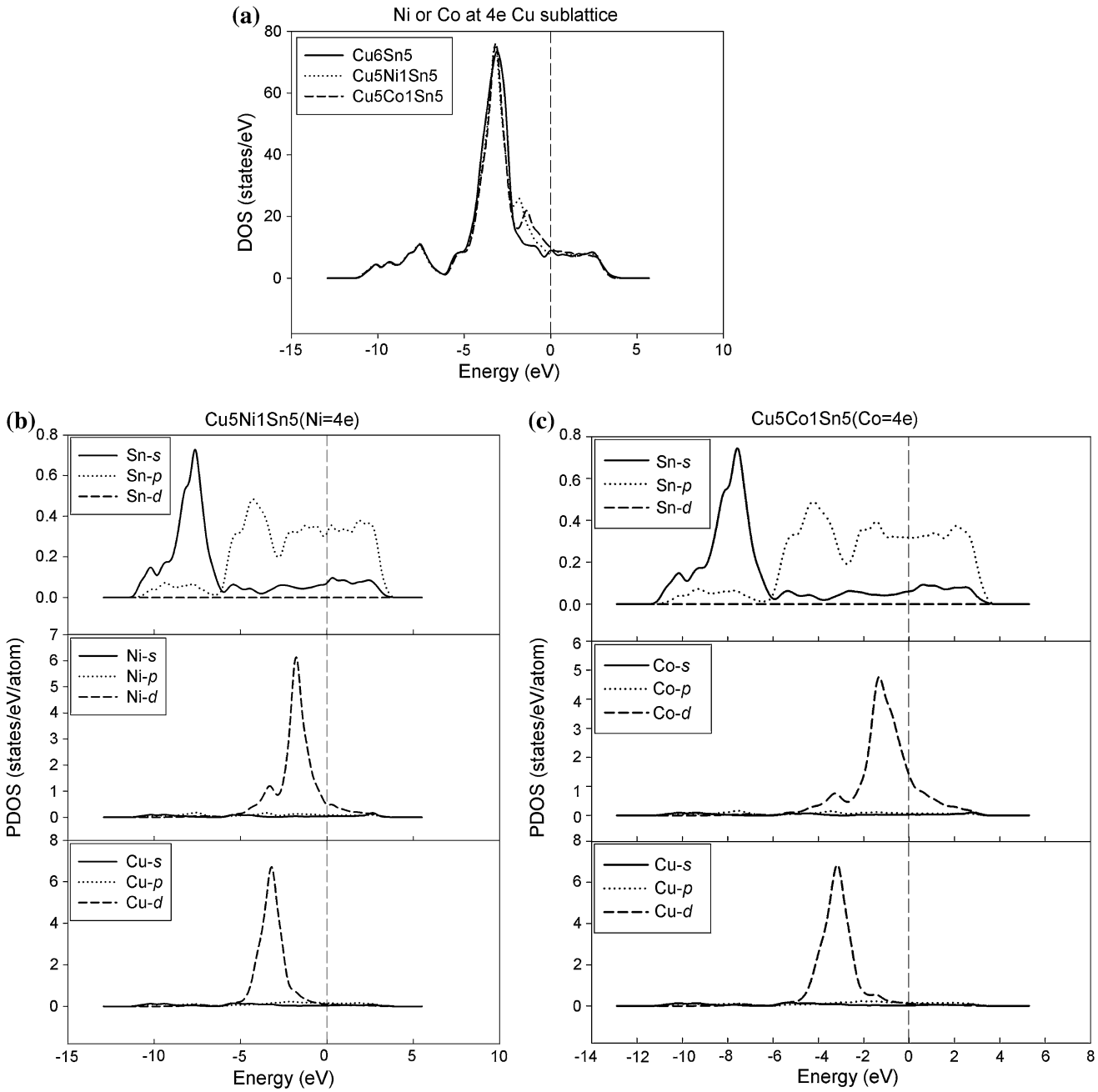

Fig. 3. Density of states (DOS) of Cu_6Sn_5, $Cu_5Ni_1Sn_5$, and $Cu_5Co_1Sn_5$ with Ni or Co occupancy at the 4e Cu sublattice: (a) total DOS comparison of Cu_6Sn_5, $Cu_5Ni_1Sn_5$, and $Cu_5Co_1Sn_5$; (b) PDOS of the Cu, Ni, and Sn states in $Cu_5Ni_1Sn_5$; (c) PDOS of the Cu, Co, and Sn states in $Cu_5Co_1Sn_5$.

hybridization between Ni-*d* and Sn-*p* states is enhanced because of the stronger Ni-*d* state PDOS than that in $Cu_5Ni_1Sn_5$. For the $Cu_4Co_2Sn_5$ phase, although the amplitude of the Co-*d* state is enhanced due to the increased Co concentration, the hybridization between Co-*d* and Sn-*p* states is reduced, as the Co-*d* state peak position mainly corresponds to the valley position of the Sn-*d* state, as shown in Fig. 4c. In addition, the total DOS value of $Cu_4Ni_2Sn_5$ at the Fermi level is also much lower than that of $Cu_4Co_2Sn_5$, as illustrated in Fig. 4a. Overall, the $Cu_4Ni_2Sn_5$ phase still exhibits higher stability than that of $Cu_4Co_2Sn_5$, where the dopants occupy the 8f2 Cu sublattice.

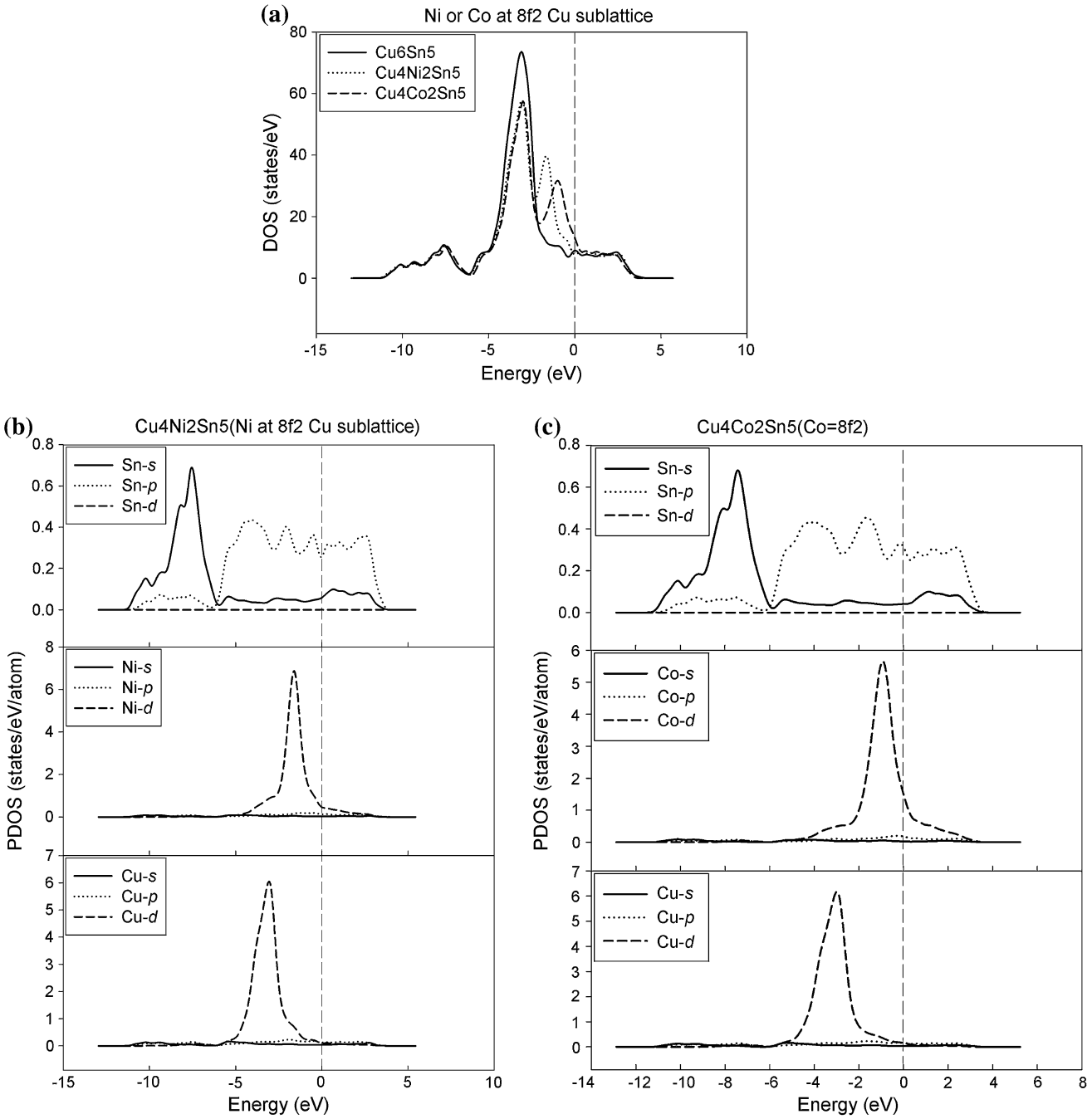

Fig. 4. Density of states (DOS) of Cu_6Sn_5, $Cu_4Ni_2Sn_5$, and $Cu_4Co_2Sn_5$ with Ni or Co occupancy at the 8f2 Cu sublattice: (a) total DOS comparison of Cu_6Sn_5, $Cu_4Ni_2Sn_5$, and $Cu_4Co_2Sn_5$; (b) PDOS of the Cu, Ni, and Sn states in $Cu_4Ni_2Sn_5$; (c) PDOS of the Cu, Co, and Sn states in $Cu_4Co_2Sn_5$.

CONCLUSIONS

Using a first-principles approach based on density-functional theory, the thermodynamic and electronic stability of Cu_6Sn_5-based phases with Ni or Co occupancy at the Cu sublattice were investigated. The following conclusions can be drawn:

(1) It follows from the calculated heats of formation that Ni or Co occupancy at the Cu sublattice in Cu_6Sn_5 leads to a more thermodynamically stable phase than Cu_6Sn_5, regardless of site occupancy. Ni occupancy is more effective at stabilizing the phase than is Co occupancy. The simulation results also show that the preferred occupancy site is 4e for the $Cu_5X_1Sn_5$ phases and 4e + 8f2 for the $Cu_3X_3Sn_5$ (X = Ni or Co) phase. Furthermore, the most favorable occupancy site is the 8f1 Cu sublattice in $Cu_4Co_2Sn_5$.

For $Cu_4Ni_2Sn_5$, although the 8f2 Cu sublattice may be more likely to be occupied by the Ni atoms, the difference from other Cu sublattices (8f1 or 4a + 4e) is not significant.

(2) The DOS and PDOS simulation results show that hybridization between Ni-*d* (or Co-*d*) and Sn-*p* states plays a dominant role in the electronic stability of the Cu_6Sn_5-based phases. For the $Cu_5Ni_1Sn_5$ and $Cu_5Co_1Sn_5$ phases where dopants occupy the 4e Cu sublattice, strong hybridization between Ni-*d* (or Co-*d*) and Sn-*p* states is observed. $Cu_5Co_1Sn_5$ is believed to be less stable than $Cu_5Ni_1Sn_5$ because of the smaller amplitude of the Co-*d* PDOS peak and the higher total DOS value of $Cu_5Co_1Sn_5$ at the Fermi level. The $Cu_4Ni_2Sn_5$ phase with Ni occupancy at the 8f2 Cu sublattice tends to be more stable due to the enhanced hybridization between Ni-*d* and Sn-*p* states. The electronic structure stability of the $Cu_4Co_2Sn_5$ phase is reduced due to the mismatch of the peak positions of the Sn-*p* and Ni-*d* states, as well as the significant increase of the total DOS value at the Fermi level.

REFERENCES

1. F. Gao, H. Nishikawa, and T. Takemoto, *J. Electron. Mater.* 36, 1630 (2007).
2. C.-H. Lin, S.-W. Chen, and C.-H. Wang, *J. Electron. Mater.* 31, 907 (2002).
3. S.-W. Chen, S.-H. Wu, and S.-W. Lee, *J. Electron. Mater.* 32, 1188 (2003).
4. G. Ghosh, *Acta Mater.* 49, 2609 (2001).
5. G. Ghosh, *J. Electron. Mater.* 33, 229 (2004).
6. T. Laurila, V. Vuorinen, and J.K. Kivilahti, *Mater. Sci. Eng. R* 49, 1 (2005).
7. W.C. Luo, C.E. Ho, J.Y. Tsai, Y.L. Lin, and C.R. Kao, *Mater. Sci. Eng. A* 396, 385 (2005).
8. L.H. Xu and J.H.L. Pang, *Thin Solid Films* 504, 362 (2006).
9. S.-W. Chen and C.-H. Wang, *J. Mater. Res.* 21, 2270 (2006).
10. V. Vuorinen, T. Laurila, T. Mattila, E. Heikinheimo, and J.K. Kivilahti, *J. Electron. Mater.* 36, 1355 (2007).
11. C.E. Ho, S.C. Yang, and C.R. Kao, *J. Mater. Sci: Mater. Electron.* 18, 155 (2007).
12. V. Vuorinen, H. Yu, T. Laurila, and J.K. Kivilahti, *J. Electron. Mater.* 37, 792 (2008).
13. F. Gao, T. Takemoto, and H. Nishikawa, *J. Electron. Mater.* 35, 2081 (2006).
14. A. Kowalczyk, M. Falkowski, V.H. Tran, and M. Pugaczowa-Michalska, *J. Alloy. Compd.* 440, 13 (2007).
15. C. Jiang, D.J. Sordelet, and B. Gleeson, *Acta Mater.* 54, 1147 (2006).
16. G. Ghosh and M. Asta, *J. Mater. Res.* 20, 3102 (2005).
17. N.T.S. Lee, V.B.C. Tan, and K.M. Lim, *Appl. Phys. Lett.* 88, 031913-1 (2006).
18. C. Yu, J.Y. Liu, H. Lu, P.L. Li, and J.M. Chen, *Intermetallics* 15, 1471 (2007).
19. N.T.S. Lee, V.B.C. Tan, and K.M. Lim, *Appl. Phys. Lett.* 89, 131908-1 (2006).
20. J. Chen and Y.-S. Lai, *Microelectron. Reliab.* 49, 264 (2009).
21. A.-K. Larsson, L. Stenberg, and S. Lidin, *Acta Crystallogr. B* 50, 636 (1994).
22. S.J. Clark, M.D. Segall, C.J. Pickard, P.J. Hasnip, M.J. Probert, K. Refson, and M.C. Payne, *Z. Kristallogr.* 220, 567 (2005).
23. *Materials Studio Version 4.4* (San Diego, CA: Accelrys, 2008).
24. A. Gangulee, G.C. Das, and M.B. Bever, *Metall. Trans.* 4, 2063 (1973).
25. J.-H. Shim, C.-S. Oh, B.-J. Lee, and D.N. Lee, *Z. Metallkd.* 87, 205 (1996).
26. K.W. Moon, W.J. Boettinger, U.R. Kattner, F.S. Biancaniello, and C.A. Handweker, *J. Electron. Mater.* 29, 1122 (2000).
27. X.J. Liu, C.P. Wang, I. Ohnuma, R. Kainuma, and K. Ishida, *Metall. Mater. Trans.* 35A, 1641 (2004).
28. G. Ghosh, *Metall. Mater. Trans.* 40A, 4 (2009).
29. T. Hong, T.J. Watson-Yang, A.J. Freeman, T. Oguchi, and J.H. Xu, *Phys. Rev. B* 41, 12462 (1990).